CrossMark

SCIENTIFIC ARTICLE

Prospective pilot study of CT-guided microwave ablation in the treatment of osteoid osteomas

Clara Prud'homme[1] · Jean-Philippe Nueffer[1] · Michel Runge[1] · Jonathan Dubut[1] ·
Bruno Kastler[1,2] · Sébastien Aubry[1,3]

Abstract

Purpose The aims of this work were to assess the feasibility and efficacy of CT-guided microwave ablation (MWA) in the treatment of osteoid osteomas (OOs).

Materials and methods Thirteen consecutive patients (range 11–31 years old) presenting with OO were prospectively included and treated by CT-guided MWA. Power and duration of MWA were both recorded. The patient's pain was assessed using a numeric pain rating scale (NRS), and side effects were recorded during procedures, after 1 day, 7 days and 1 month. The nidus vascularization and the volume of necrosis induced by MWA were assessed using contrast-enhanced MRI. Success was defined as the complete relief of the patient's pain 1 month after the first procedure, associated with necrosis of the nidus on follow-up MRI.

Results The success rate was up to 92.3% (12/13). At 1 day, 7 days and 1 month, the median NRSs were respectively 5 [interquartile range (IQR) 2–5], 0 (IQR 0–1) and 0 (IQR 0–0). Side effects observed were one partial and self-resolving lesion of a sensory branch of the radial nerve and two skin burns. The median power of the MWA used was 60 W (IQR 50–60) with a 1.5-min duration (IQR 1–2), leading to MWA-induced necrosis measuring on average 23 × 15 × 16 mm.

Conclusion CT-guided MWA of OO has a success rate that appears to be almost similar to that of laser or radiofrequency ablation, but care must be taken to prevent nerve or skin lesions.

Keywords Osteoid osteoma · Microwave ablation ·
CT-guided procedure · Thermoablation · Treatment · Efficacy

Introduction

Osteoid osteoma (OO) is a benign osteoblastic tumor, representing 2 to 3% of all bone tumors and approximately 13.5% of all benign bone tumors [1]. These small tumors (usually of <1.5 cm diameter) have a minimal or non-existant growth rate. Histologically, OO is composed of a small hypervascular central nidus, surrounded by a fibrovascular rim and a purely reactive sclerosis. It causes paroxysmal nocturnal pain and produces high levels of prostaglandins, especially PGE2 and PGI2 [2]. For this reason, this type of tumor is typically sensitive to salicylates. It preferentially sits on the shaft of a long bone and affects young patients (sex ratio male/female = 2) aged between 10 and 30 years. Only destruction of the nidus ensures a permanent cure.

A few decades ago, surgery was the standard therapy for OO and was successful in 90% of all cases. However, there were complications such as fractures due to too large a volume of bone resection. Today, image-guided radiofrequency ablation (RFA) is considered to be the new gold standard for the treatment of OO. This minimally invasive procedure is widely available, safe and effective [3–8], although the recurrence rate after RFA has been reported to be from 5 to 10% [8–11]. Its efficacy may be limited by high impedance inside the OO [12]. Nonetheless, microwave ablation (MWA) presents specific advantages over RFA, namely lower sensitivity

✉ Sébastien Aubry
   radio.aubry@free.fr

1   Department of Musculoskeletal Imaging, University Hospital of
    Besancon, 25000 Besancon, France

2   I4S Laboratory, INSERM EA4268, University of Franche-Comte,
    25000 Besancon, France

3   Nanomedecine Laboratory, INSERM EA4662, University of
    Franche-Comte, 25000 Besancon, France

to variations in tissue composition, tissue carbonization and bone impedance, with the result that MWA achieves higher temperatures within the tumor more quickly [13]. Therefore, MWA may be used to avoid increased impedance, which may limit the energy deposit during RFA in sclerotic bone lesions [14–16].

To the best of our knowledge, only two pilot studies of MWA for OO have previously been published, namely by Kostrzewa et al. [17] and Basile et al. [18]. Basile et al. included seven patients and only epiphyseal lesions located at 2 cm within the bone to avoid complications. Kostrzewa's study aimed to demonstrate the feasibility of MWA in the treatment of OO located only on the lower limb in ten patients.

The current prospective pilot study was designed to assess the feasibility and outcome of CT-guided percutaneous MWA performed at a single institution in a consecutive series of patients with OO located in the appendicular skeleton. The objectives of this study were therefore (1) to briefly describe the technique used, (2) to assess tolerance and (3) to evaluate the short-term efficacy.

Materials and methods

This study was approved by the local Ethics Committee and by the **blinded** Health Products Safety Agency. Written informed consent was obtained from all adult patients. Written informed consent was obtained from the subject's parent or guardian if the patient was a minor.

The inclusion criteria were:

–   A painful bone lesion whose CT scan appearance was a focal lucent nidus <2 cm in size, with or without a central sclerotic dot, within surrounding sclerotic reactive bone, consistent with an OO;
–   Patients referred to our institution by their physician for percutaneous thermoablation;
–   Signature of the informed consent form stating that the patient, or parent or guardian if the patient was a minor, understood the aims of the study and the procedure.

Exclusion criteria were as follows:

–   Spinal OO;
–   Contraindication to percutaneous thermo-ablation, namely coagulation disorders (prothrombin ratio <60%, aPTT >60 s, platelet count <150,000/mm^3);
–   Pregnancy;
–   Patients with no social security coverage.

Thirteen consecutive patients were included in the study, and none were excluded, between July 2013 and March 2016: Ten males and three females (sex ratio male/female = 3.33)

ranging from 11 to 31 years of age (median 21, IQR 17–23). Pain lasted for 18 months (IQR 12–24) and was scored 7 (IQR 6–7). The median nidus diameter was 5.7 mm (IQR 5–7). OO was located in the femur ($n = 6$), tibia ($n = 3$), talus ($n = 2$), radius ($n = 1$) and scapula ($n = 1$) (Table 1). In 10 out of 13 cases, the diagnosis of OO was histologically confirmed. In the remaining three, histological analysis indicated non-specific osteosclerosis.

All procedures were performed using a Siemens Sensation 64 CT scan (Siemens Healthcare, Erlangen, Germany) in the prone or supine position depending on the position of the lesion. Initially, patients could choose to undergo MWA under local anesthesia or under general or epidural anesthesia. The arguments in favor of local anesthesia were the good tolerance of the technique as described by Kastler et al. [19] in MWA of spinal metastatic bone tumors during MWA lasting up to 8 min. Patients were informed that they would feel some pain that might be intense for a relatively short time (1.5 to 2 min). This might seem bearable and would avoid the potential side effects of general anesthesia or an epidural. Accordingly, the first five patients chose to undergo thermoablation under local anesthesia. In those cases, 1 g of acetaminophen (Rotexmedica®, Trittau, Germany) was injected intravenously in addition to an equimolar mixture of oxygen-nitrous oxide (EMONO) inhaled through a mask (9–12 l/min, patient-controlled, Kalinox®, Air Liquide Sante International, Paris, France). In these patients, the pain felt during the initial step of biopsy and/or the heating step was widely variable, unpredictable and, in some cases, unbearable. It caused some patients to move, disturbing the operator. Thus, a protocol amendment was implemented to perform the eight subsequent procedures under general (7 patients) or epidural anesthesia (1 patient). The choice between those two methods was made by consensus between the patients and the anesthesist during a dedicated pre-anesthetic consultation.

The target lesion and needle path were located through non-enhanced helical CT acquisitions (Fig. 1a). After accurate marking of the skin and in strictly aseptic conditions, local subcutaneous injection of lidocaine 1% (Xylocaine®, Abbott, Chicago, IL, USA) was performed at the defined skin entry point. When the procedure was performed under local anesthesia, a 22-gauge needle was introduced step by step under CT fluoroscopy, and lidocaine anesthesia was performed through the pathway, from the entry point to periosteum. The bone was perforated using an 11-G bone trocar (included in a t'CDII Kit, Thiebaud®, Margencel, France). Coaxial biopsy was performed with a 13-G trephine bone marrow biopsy needle (also included in the t'CDII Kit, Thiebaud®, Margencel, France) (Fig. 1b). When the procedure was performed under local anesthesia, lidocaine hydrochloride (1%, 1 cc) was slowly injected in the path of the biopsy through the bone trocar. The thermoablation antenna (in 12 cases an Acculis® Generator, Angiodynamics, Latham,
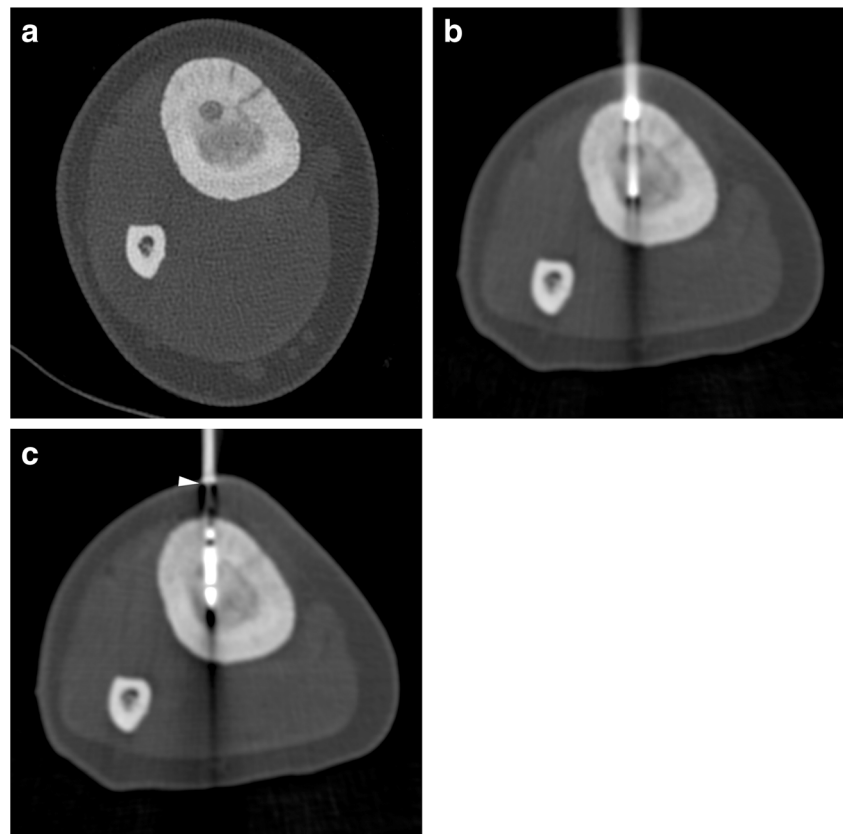
Table 1   Detailed results concerning the location of 13 consecutively included osteoid osteomas, symptom duration before the procedure, power and duration of MWA, size of MWA-induced necrosis and peripheral scar, success and numeric pain rating scale (NRS) scores before, during the procedure (D0) and after 1 day (D1), 7 days (D7) and 1 month (M1)

Pat. no.	Age (years old)	Location	Symptom duration before procedure (months)	MWA (Watt, min)	Length, width, thickness of necrosis (mm)	Thickness of peripheral scar (mm)	Success	NRS (before, D0, D1, D7, M1)
1	20	Femur	24	60 W, 2 min	23, 12, 14	3	Yes	9, 0, 0, 0, 0
2	19	Tibia	18	60 W, 2 min	24, 18, 19	3	Yes	7, 0, 7, 0, 0
3	21	Radius	24	50 W, 1 min	17, 9, 9	1.5	Yes	6, 9, 6, 1, 0
4	28	Talus	18	60 W, 1 min	20, 15, 16	3	Yes	7, 6, 5, 0, 0
5	21	Talus	18	50 W, 1 min	14, 7, 8	2.5	No	8, 10, 5, 6, 6
6	31	Scapula	12	50 W, 1 min	27, 20, 19	2	Yes	5, 5, 5, 0, 0
7	21	Femur	24	50 W, 2 min	22, 16, 18	2.5	Yes	4, 0, 0, 0, 0
8	11	Femur	9	60 W, 2.5 min	26, 21, 23	2	Yes	7, 1, 2, 0, 0
9	15	Tibia	12	60 W, 1.5 min	24, 14, 15	3.5	Yes	4, 0, 0, 0, 0
10	16	Femur	24	60 W, 1.5 min	24, 17, 20	3.5	Yes	7, 1, 2, 0, 0
11	26	Femur	21	60 W, 1.5 min	22, 17, 17	2	Yes	6, 0, 4, 0, 0
12	23	Tibia	24	60 W, 1.5 min	18, 14, 14	3	Yes	7, 0, 5, 3, 0
13	17	Femur	12	60 W, 1.5 min	23, 15, 15	2.5	Yes	7, 0, 6, 1, 0

NY, USA, and in one case an AMICA® generator, Ablatech, Toulouse, France) was coaxially introduced into the trocar. The bone trocar was then partially removed (2 cm) to avoid contact between the active tip of the MWA probe and the trocar (Fig. 1c). MWA was then performed, adapting the power settings and ablation time to the size of the lesions and, in

the absence of recommendations from the constructor, based on our 2-year experience in the treatment of bone and soft tumors by MWA. Adjunct maneuvers were used to protect non-target anatomy, such as the skin: hence, saline solution was injected under the skin to pull it back from the bone when the hypodermis was too thin. Full weight-bearing was allowed

Fig. 1 **a** Axial CT scan of a subcortical osteoid osteoma. **b** Coaxial biopsy of the nidus under CT control. **c** Axial CT control before MWA ablation. The active tip of the microwave probe is centered on the nidus. The bone trocar was removed to the skin (*arrowhead*) to avoid contact with the active tip of the probe

on the evening of the procedure, but sport and physical activities were contraindicated for a 1-month period.

Imaging follow-up and data recording

We used a numeric pain rating scale (NRS) to assess the patient's pain during a medical consultation (i.e., with the physician) at each timepoint during the study. Patients were asked to make a rating corresponding to the worst pain experienced over the past 24 h and to circle the number that best represented their pain intensity on an 11-point scale ranging from 0 to 10, where 0 corresponds to no pain and 10 corresponds to the worst possible pain (Fig. 2).

The following data were recorded by the main investigator (SA) for each patient:

- Patient and lesion characteristics assessed prior to the procedure: age, sex, lesion site and nidus size. The maximum level of pain experienced by the patient during the month prior to the procedure was assessed by NRS. The duration of pain prior to the procedure (in months) was also recorded.
- Start time and finish time of the procedure as well as the duration and power of thermoablation.
- Tolerance was assessed by recording the maximal rating (out of 10) on an NRS during the procedure and recording any adverse effects.
- Pain relief was assessed by NRS at 1 day, 7 days and 1 month after the procedure.
- The treated lesions were followed up at 1 month by dynamic contrast-enhanced MRI (Siemens Aera 1.5T, Erlangen, Germany). The protocol was adapted according to the bone lesion site, but in all cases included at least one T1-weighted sequence, one short tau inversion recovery or fat-suppressed T2-weighted sequence, one dynamic contrast-enhanced 3D gradient-echo T1-weighted sequence and one contrast-enhanced fat-suppressed T1-weighted sequence. We measured the length, width, thickness and volume of microwave-induced necrosis and the thickness of the high-signal surrounding microwave-induced necrosis, and we checked for the absence of a contrast-enhancing nidus (i.e., nidus necrosis) (Fig. 3).
- The distance between the probe and the nidus center was measured on the CT images performed during the procedure and checked on the follow-up MRI.

MWA success was defined as total pain relief associated with necrosis of the nidus on the follow-up MRI.

Statistical analysis

After verifying coherence and data quality, descriptive analysis was performed to analyze the effect of MWA. Qualitative variables are expressed as number and percentage and quantitative variables as median and interquartile range (IQR). All analyses were performed using SAS version 9.3 (SAS Institute Inc., Cary, NC, USA).

Results

From the first puncture to antenna withdrawal, MWA procedures were performed in a median time of 35 min (IQR 28–44). The median power of MWA used was 60 W (IQR 50–60), with a 1.5-min duration (IQR 1–2), leading to MWA-induced necrosis measuring on average $23 \times 15 \times 16$ mm (2.69 cm^3), surrounded by a 2.6-mm-thick high signal (IQR 2–3). Detailed results of the size of the necrosis as a function of power and duration are presented in Table 2. The distance between the probe and the nidus was zero in all but two cases: in the first case, a nidus of the talus was located 4 mm inferior to the probe on the MRI, yet we believed that the needle placement was accurate based on CT images performed during the procedure. As the control images were 5 mm thick, this error was due to a partial volume effect, associated with a slight movement of the ankle during the procedure. In the second case, the nidus was difficult to reach at the inferior aspect of the femoral neck, and the center of the nidus was 3 mm posterior to the probe.

Median NRS during the procedures was 0 (IQR 0–6). However, no pain was felt in the subgroup of patients treated under general anesthesia or epidural anesthesia, whereas in the subgroup of patients treated under local anesthesia combined with EMONO, median NRS was 9 (IQR 6–9.8). Moreover, the total duration of the procedures was shorter under general or epidural anesthesia (median = 34.5 min) than under local anesthesia (median = 44 min). Median NRS was 5 (IQR 2–5) after 1 day and 0 (IQR 0–1) after 7 days. After 1 month, 12 patients experienced total pain relief, and 1 patient had an NRS of 6, so that the median NRS for the whole sample was 0 (IQR 0–0) (Fig. 4). The procedural failure was observed in a 5.3-mm OO located in the talus and treated under local anesthesia by MWA for 1 min at 50 W. The MRI follow-up

Fig. 2 A 0–10 numeric pain rating scale used as a pain assessment tool during the study

0 1 2 3 4 5 6 7 8 9 10

No pain   **Moderate pain**   **Worst possible pain**

Fig. 3 a One-month MRI follow-up of a femoral osteoid osteoma. The nidus is invisible. The length and height of the low-signal MWA-induced necrosis were measured on this coronal image (*white arrows*). Moderate, asymptomatic synovitis is visible (*black arrowhead*). **b** Anteroposterior dimension of the necrosis was measured and a reformatted sagittal image from a 3D gradient echo T1-weighted acquisition (*white arrow*). Necrosis is surrounded by an enhancing high-signal peripheral scar (*white arrowhead*)

revealed that the probe was 4 mm away from the center of the nidus, that the nidus was located in the high-signal surrounding necrosis and that it was still contrast enhancing (Fig. 5). In all other cases, the MWA-induced necrosis fully comprised the OO. Consequently, the overall success rate was 92.3% (12/13).

Some complications were observed. One patient, treated for an OO located within the distal third of the left radius, had a partial and self-resolving lesion of a sensory branch of the radial nerve, as well as a moderate skin burn (grade 2) after MWA treatment at 50 W for 1 min. Another patient had a grade 3 skin burn after the treatment of a tibial OO (60 W for 1 min 30) despite hydrodissection between the skin and the anterior tibia. This resulted in a rate of 15.3% grade B complications according to the SIR classification [20].

Discussion

OO causes paroxysmal nocturnal pain, typically sensitive to salicylates. The time between the onset of pain and treatment is typically long and is related to the non-specificity of symptoms, the latency between the onset of symptoms and the appearance of the lesion on radiological studies, and the evaluation sequence used in some patients [21]. The mean duration between the onset of symptoms and CT identification of an OO was estimated to be 26 months (range: 6–42 months) [22], which is consistent with our observations (18 months).

Some authors assume that OOs heal spontaneously. In the study by Kneisl, the authors concluded that long-term administration of non-steroidal antiinflammatory drugs can often be as effective as surgical excision for the treatment of OO [23]. However, when pain persists for several months, image-guided thermo-ablation is recommended. RFA is currently the most widely used technique [9, 24], because it leads to high pain reduction rates (up to 96%) and low recurrence rates (around 7% after 2 years) [25, 26]. As suggested by the promising results of a few retrospective studies [27, 28], the potential benefits of MWA compared to RFA are its efficiency, speed and safety.

Our study confirms the excellent curative potential of MWA, with a success rate reaching 92.3%. This is similar to some reports on RFA, whose reported primary success rate has been reported at 78.2% [26], 91% [7] and 94% [8] depending on the study. Recently, it appeared that RFA could reach 100% efficacy [29] thanks to technical optimizations such as the dual-cycle RFA technique [30]. It seems possible—and necessary—that MWA should also benefit from technical improvements to achieve this objective.

Our results are consistent with two preliminary studies that evaluated MWA in the treatment of OO [17, 18]. In the study by Kostrzewa et al., all patients were pain-free within 1 week after their intervention, and there were no recurrences during the 6 months of follow-up. Similarly, in the study by Basile et al., all patients experienced resolution of symptoms (NRS <1 without medication) until their last follow-up, with

**Table 2** Mean size of MWA-induced necrosis as a function of power and time

	1 min	1 min 30	2 min	2 min 30
50 W	19.3 × 12 × 12 mm (*n* = 3)		22 × 16 × 18 mm (*n* = 1)	
60 W	20 × 15 × 16 mm (*n* = 1)	22.2 × 15.4 × 16.2 mm (*n* = 5)	23.5 × 15 × 16.5 mm (*n* = 2)	26 × 21 × 23 mm (*n* = 1)

Fig. 4 Clinical follow-up of the pain. Median (interquartile range), minimum (Min) and maximum (Max) numeric pain rating scale (NRS) values before and during (D0) MWA and at 1 day (D1), 7 days (D7) and 1 month (M1) after MWA
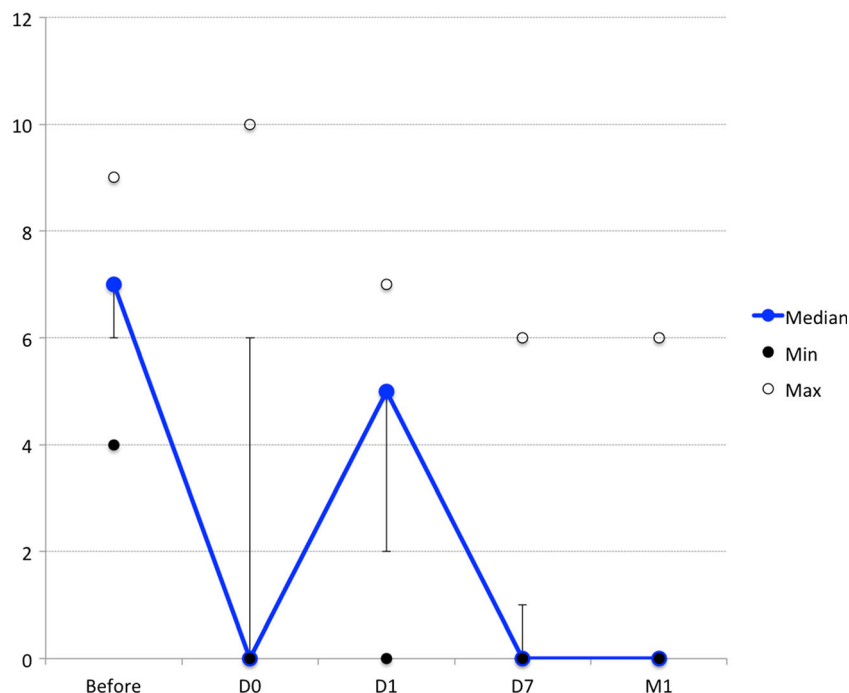
residual NRS <2 occurring only from 1 to 7 days after the procedure. The high NRS value after 1 day (median NRS = 5) is influenced by post-procedure pain. We managed it with a patient-controlled oral analgesia that associated grade 2 analgesics with a nonsteroidal antiinflammatory drug for 3 days on the postoperative course following MWA (two acetaminophen-codeine 500 mg/30 mg and one ibuprofen
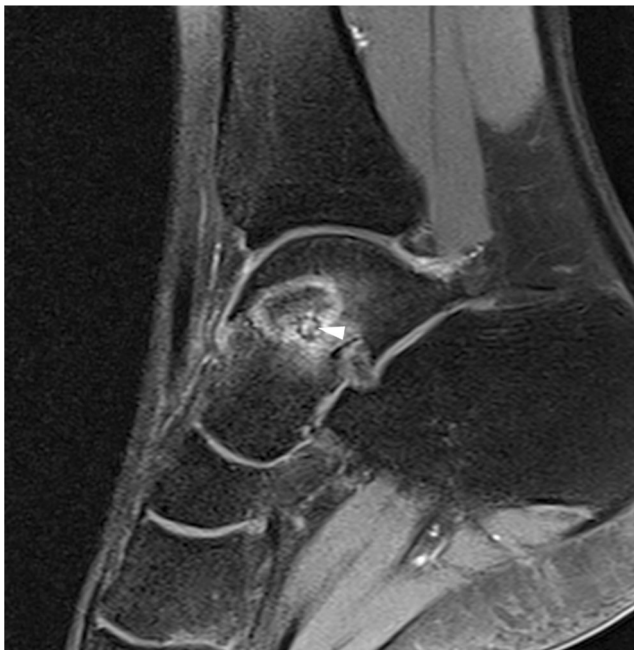
Fig. 5 One-month follow-up MRI of an osteoid osteoma of the talus. The nidus (*arrowhead*) is located in the peripheral high signal scar under the MWA-induced necrosis and is still enhanced. There is also a moderate bone marrow edema around the residual osteoid osteoma

400 mg three times a day). The only failure in our series was observed in one case of suboptimal treatment and was due to several reasons. The patient was treated under local anesthetic and inhalation of EMONO. The pain induced by the positioning of the probe and by the thermoablation itself was substantial. Consequently, the power and duration of the MWA had to be reduced. In addition, we noticed on control (Fig. 5) that the probe was not accurately placed at the center of the nidus. Patients who were treated under local anesthesia and inhalation of EMONO had a grossly unsatisfactory experience because of the very high pain scores during the procedures (median NRS = 9 in that subgroup). Consequently, we recommend epidural or general anesthesia for all cases. With adequate anesthesia, patients felt no pain and did not move during the procedures. This situation explains why the duration of our procedures was shorter under general or epidural anesthesia.

For such a small group of patients, to have observed three complications is not insignificant, even grade B events. The use of adjunct maneuvers (subcutaneous CO_2 pneumodissection or hydrodissection), as previously described in cryoablation and RFA [31, 32], might have prevented the occurrence of one skin burn. However, in the other case, hydrodissection was not enough because the length of the treated area was too long. New thermoreversible hydrogel can also protect non-target tissues adjacent to MWA, but they are not yet approved for clinical use [33]. No side effects have been reported heretofore because only epiphyseal OOs of long bones were selected in one study [18], and in the other available study, lower power (16 W) and duration (60 s) were used [17]. As a precaution, we recommend a margin of 1 cm between the ablation zone and untargeted body elements such as nerves and skin. This is why

we excluded spinal OO. In such particularly risky locations, laser ablation may be used [34].

MWA allows temperatures to rise faster (up to 170 °) compared to RFA because of fewer impedance limitations [13, 35]. The organs that seem most amenable to destruction by microwaves are those that have a high permittivity difference between tumors and surrounding tissues. Thus, treatment of OO located in the appendicular skeleton can be achieved more quickly, even in sclerosing lesions. From the first puncture to the withdrawal of the antenna, MWA can be done in approximately half an hour. A few minutes are saved as a result of the short period of time that is needed for the treatment (1.5 min) in comparison to the time required for RFA. Most authors perform RFA by controlling the temperature, reaching 90° at the forefront for 4–6 min [36]. Vanderschueren et al. stated that the use of only one RF needle was the most important independent parameter associated with an increased risk of treatment failure [37]. However, multiple needle insertions lead to an increase in procedural time and radiation exposure. It results in a total duration of RFA varying from 45 to 120 min [36].

Another consequence of the physical properties of MWA is an increased homogeneous volume of thermal ablation compared to RFA. In addition, it appears that the ablation regions are more spherical [38] and have a single impact of microwaves, which achieve a transverse diameter of about 3.5 cm. RFA techniques described for the treatment of OO include the use of monopolar or bipolar RF electrodes and plasma-mediated RF electrodes [39, 40]. Since the maximum diameter of the lesion with a single uncooled electrode is 16 mm, then the end of the probe must be positioned at the center of the lesion. If the tumor grows more than 5 mm on each side of the probe, a reset and a second treatment should be performed. Theoretically, unlike with RFA, MW antennae and cryoprobes do not need to be placed perfectly at the center of the nidus. This could be helpful when lesions are not perfectly visible or with lesions presenting thick osteosclerosis, which is difficult to overcome. One of the advantages of microwave therapy is that it offers, as does cryoablation, the possibility of cortical crossing [41, 42], although in these cases, it becomes necessary to increase the power and the duration of treatment to extend the size of the area of treatment, with an increased risk of damage to sensitive adjacent structures, such as the skin or nerves. Given the size of the lesions treated in our study, our aim was to limit the diameter of the necrotic area to 15 mm. We observed that for a shorter processing time (1.5 min), the area of necrosis induced by microwaves presented itself as homogeneous and ovoid, and the peri-wound scar in high signal appeared thin (<3 mm). However, for a short time and low power, while the diameter of the treated area decreased, its length remained at least 19 mm. Ideally, microwave probes having a shorter active tip would be necessary to generate small spherical ablation zones, as cryoablation does.

Since the necrosis induced by MWA is potentially large, good knowledge of the size of the necrotic zone over time is mandatory. We were able to establish a table tracing the size of the necrotic zone over time, as a function of the initial duration and power of ablation (Table 2). To the best of our knowledge, given that there was no reliable CT monitoring of the necrotic zone during the procedure, information of this sort is highly useful as a guide for operators. The very high temperatures achieved by MWA cause outgassing, so that the post-ablation area on CT may contain several small gas bubbles of various sizes that are distributed in the ablated tissue, creating a "gas cloud." These gas bubbles do not seem to be a precise marker, because both under- and over-estimations of the true extent of coagulation have been reported [43]. Furthermore, in our experience, we have never observed outgassing after MWA of OO. The post-ablative hypo-attenuating area was found to correlate with the volume of ablated liver tissue, but this has never been assessed on ablated bone tissue [44]. Only MR thermometry directly evaluates the extent of heat, which requires performing MWA under MR control. Further data are warranted from larger study populations, testing different power and duration combinations with various commercially available MWA systems.

Our study suffers from some limitations related to the small size of our population, although it remains the largest prospective case series to date. Also, lesions of the axial skeleton were excluded. In this rare localization, the use of thermocouples, hydrodissection and carbodissection may prevent the occurrence of side effects so that the intervention can be envisaged. However, we currently do not recommend using MWA in the treatment of OO located in the neural arch. We only assessed the short-term efficacy (1 month). It would be interesting to obtain long-term follow-up beyond 6 months. Finally, we did not evaluate the economic impact of MWA, which is currently more expensive than RFA [respectively, approximately 700 euros (770 USD) versus 1300 euros (1430 USD) per probe].

Conclusion

CT-guided MWA is effective in the treatment of OO of the appendicular skeleton and should always be performed under general or epidural anesthesia, but this remains to be confirmed in longer term studies and with larger populations. CT-guided MWA of OO has a success rate that appears to be almost similar to that of laser or radiofrequency ablation, but care must be taken to prevent nerve or skin lesions.

Ethical approval All procedures performed in studies involving human participants were in accordance with the ethical standards of the institutional and/or national research committee and with the 1964 Helsinki Declaration and its later amendments or comparable ethical standards.

References

1. Dahlin DC, Unni KK. Bone tumors: general aspects and data on 8,542 cases. Springfield: Charles C Thomas Pub Ltd; 1986. p. 88–101.

2. Greco F, Tamburrelli F, Ciabattoni G. Prostaglandins in osteoid osteoma. Int Orthop. 1991;15(1):35–7.

3. Filippiadis DK, Tutton S, Mazioti A, Kelekis A. Percutaneous image-guided ablation of bone and soft tissue tumours: a review of available techniques and protective measures. Insights Imaging. 2014;5(3):339–46.

4. Moser T, Buy X, Goyault G, Tok CH, Irani F, Gangi A. Image-guided ablation of bone tumors: review of current techniques. J Radiol. 2008;89(4):461–71.

5. Lindner NJ, Ozaki T, Roedl R, Gosheger G, Winkelmann W, Wörtler K. Percutaneous radiofrequency ablation in osteoid osteoma. J Bone Joint Surg (Br). 2001;83(3):391–6.

6. Vanderschueren GM, Taminiau AHM, Obermann WR, Bloem JL. Osteoid osteoma: clinical results with thermocoagulation. Radiology. 2002;224(1):82–6.

7. Rosenthal DI, Hornicek FJ, Torriani M, Gebhardt MC, Mankin HJ. Osteoid osteoma: percutaneous treatment with radiofrequency energy. Radiology. 2003;229(1):171–5.

8. Woertler K, Vestring T, Boettner F, Winkelmann W, Heindel W, Lindner N. Osteoid osteoma: CT-guided percutaneous radiofrequency ablation and follow-up in 47 patients. J Vasc Interv Radiol. 2001;12(6):717–22.

9. Rosenthal DI, Springfield DS, Gebhardt MC, Rosenberg AE, Mankin HJ. Osteoid osteoma: percutaneous radio-frequency ablation. Radiology. 1995;197(2):451–4.

10. Kjar RA, Powell GJ, Schilcht SM, Smith PJ. Percutaneous radiofrequency ablation for osteoid osteoma: experience with a new treatment. Med J Aust. 2006;184(11):563–5.

11. Rehnitz C, Sprengel SD, Lehner B, et al. CT-guided radiofrequency ablation of osteoid osteoma and osteoblastoma: clinical success and long-term follow up in 77 patients. Eur J Radiol. 2012;81(11):3426–34.

12. Pinto CH, Taminiau AHM, Vanderschueren GM, Hogendoorn PCW, Bloem JL, Obermann WR. Technical considerations in CT-guided radiofrequency thermal ablation of osteoid osteoma: tricks of the trade. AJR Am J Roentgenol. 2002;179(6):1633–42.

13. de Baere T. New techniques of tumor ablation (microwaves, electroporation). J Radiol. 2011;92(9):789–95.

14. Brace CL. Microwave ablation technology: what every user should know. Curr Probl Diagn Radiol. 2009;38(2):61–7.

15. Yu J, Liang P, Yu X-L, et al. US-guided percutaneous microwave ablation of renal cell carcinoma: intermediate-term results. Radiology. 2012;263(3):900–8.

16. Durick NA, Laeseke PF, Broderick LS, et al. Microwave ablation with triaxial antennas tuned for lung: results in an in vivo porcine model. Radiology. 2008;247(1):80–7.

17. Kostrzewa M, Diezler P, Michaely H, et al. Microwave ablation of osteoid osteomas using dynamic MR imaging for early treatment assessment: preliminary experience. J Vasc Interv Radiol. 2014;25(1):106–11.

18. Basile A, Failla G, Reforgiato A, et al. The use of microwaves ablation in the treatment of epiphyseal osteoid osteomas. Cardiovasc Intervent Radiol. 2014;37(3):737–42.

19. Kastler A, Alnassan H, Aubry S, Kastler B. Microwave thermal ablation of spinal metastatic bone tumors. J Vasc Interv Radiol. 2014;25(9):1470–5.

20. Sacks D, McClenny TE, Cardella JF, Lewis CA. Society of interventional radiology clinical practice guidelines. J Vasc Interv Radiol. 2003;14(9 pt 2):S199–202.

21. Kattapuram SV, Kushner DC, Phillips WC, Rosenthal DI. Osteoid osteoma: an unusual cause of articular pain. Radiology. 1983;147(2):383–7.

22. Glanzmann MC, Imhoff AB, Schwyzer H-K. Osteoid osteoma of the shoulder and elbow: from diagnosis to minimally invasive removal. Int Orthop. 2013;37(12):2403–8.

23. Kneisl JS, Simon MA. Medical management compared with operative treatment for osteoid-osteoma. J Bone Joint Surg Am. 1992;74(2):179–85.

24. Rosenthal DI, Alexander A, Rosenberg AE, Springfield D. Ablation of osteoid osteomas with a percutaneously placed electrode: a new procedure. Radiology. 1992;183(1):29–33.

25. Rosenthal D, Callstrom MR. Critical review and state of the art in interventional oncology: benign and metastatic disease involving bone. Radiology. 2012;262(3):765–80.

26. Donkol RH, Al-Nammi A, Moghazi K. Efficacy of percutaneous radiofrequency ablation of osteoid osteoma in children. Pediatr Radiol. 2008;38(2):180–5.

27. Pusceddu C, Sotgia B, Fele RM, Melis L. Treatment of bone metastases with microwave thermal ablation. J Vasc Interv Radiol. 2013;24(2):229–33.

28. Yang X, Ye X, Zheng A, et al. Percutaneous microwave ablation of stage I medically inoperable non-small cell lung cancer: clinical evaluation of 47 cases. J Surg Oncol. 2014;110(6):758–63.

29. Miyazaki M, Arai Y, Myoui A, et al. Phase I/II multi-institutional study of percutaneous radiofrequency ablation for painful osteoid osteoma (JIVROSG-0704). Cardiovasc Intervent Radiol. 2016;39(10):1464–70.

30. Abboud S, Kosmas C, Novak R, Robbin M. Long-term clinical outcomes of dual-cycle radiofrequency ablation technique for treatment of osteoid osteoma. Skelet Radiol. 2016;45(5):599–606.

31. Maybody M, Tang PQ, Moskowitz CS, Hsu M, Yarmohammadi H, Boas FE. Pneumodissection for skin protection in image-guided cryoablation of superficial musculoskeletal tumours. Eur Radiol. 2016. doi:10.1007/s00330-016-4456-6.

32. Lee SJ, Choyke LT, Locklin JK, Wood BJ. Use of hydrodissection to prevent nerve and muscular damage during radiofrequency ablation of kidney tumors. J Vasc Interv Radiol. 2006;17(12):1967–9.

33. Moreland AJ, Lubner MG, Ziemlewicz TJ, et al. Evaluation of a thermoprotective gel for hydrodissection during percutaneous microwave ablation: in vivo results. Cardiovasc Intervent Radiol. 2015;38(3):722–30.

34. Gangi A, Alizadeh H, Wong L, Buy X, Dietemann J-L, Roy C. Osteoid osteoma: percutaneous laser ablation and follow-up in 114 patients. Radiology. 2007;242(1):293–301.

35. Deschamps F, Farouil G, de Baere T. Percutaneous ablation of bone tumors. Diagn Interv Imaging. 2014;95(7–8):659–63.

36. Okuma T, Matsuoka T, Yamamoto A, Hamamoto S, Nakamura K, Inoue Y. Assessment of early treatment response after CT-guided radiofrequency ablation of unresectable lung tumours by diffusion-weighted MRI: a pilot study. Br J Radiol. 2009;82(984):989–94.

37. Vanderschueren GM, Taminiau AHM, Obermann WR, van den Berg-Huysmans AA, Bloem JL. Osteoid osteoma: factors for increased risk of unsuccessful thermal coagulation. Radiology. 2004;233(3):757–62.

38. He N, Wang W, Ji Z, Li C, Huang B. Microwave ablation: an experimental comparative study on internally cooled antenna

versus non-internally cooled antenna in liver models. Acad Radiol. 2010;17(7):894–9.

39. Witt JD, Hall-Craggs MA, Ripley P, Cobb JP, Bown SG. Interstitial laser photocoagulation for the treatment of osteoid osteoma. J Bone Joint Surg (Br). 2000;82(8):1125–8.

40. Dasenbrock HH, Gandhi D, Kathuria S. Percutaneous plasma mediated radiofrequency ablation of spinal osteoid osteomas. J Neurointerv Surg. 2012;4(3):226–8.

41. Eshet Y, Mann RR, Anaton A, Yacoby T, Gefen A, Jerby E. Microwave drilling of bones. IEEE Trans Biomed Eng. 2006;53(6):1174–82.

42. Carrafiello G, Laganà D, Mangini M, et al. Microwave tumors ablation: principles, clinical applications and review of preliminary experiences. Int J Surg. 2008;6:S65–9.

43. Goldberg SN, Grassi CJ, Cardella JF, et al. Image-guided tumor ablation: standardization of terminology and reporting criteria. Radiology. 2005;235(3):728–39.

44. Cha CH, Lee FT, Gurney JM, et al. CT versus sonography for monitoring radiofrequency ablation in a porcine liver. AJR Am J Roentgenol. 2000;175(3):705–11.